



ELSEVIER

Available online at www.sciencedirect.com

SCIENCE @ DIRECT®

Tectonophysics 377 (2003) 249–268

TECTONOPHYSICS

www.elsevier.com/locate/tecto

Middle Paleozoic paleomagnetism of east Kazakhstan: post-Middle Devonian rotations in a large-scale orocline in the central Ural–Mongol belt[☆]

Natalia M. Levashova^a, Kirill E. Degtyarev^a, Mikhail L. Bazhenov^{a,b},
Adam Q. Collins^b, Rob Van der Voo^{b,*}

^aGeological Institute, Academy of Sciences of Russia, Pyzhevsky Lane 7, Moscow 109017, Russia

^bDepartment of Geological Sciences, University of Michigan, Ann Arbor MI 48109-1063, USA

Received 15 November 2002; accepted 2 September 2003

Abstract

In order to test different hypotheses concerning the Paleozoic evolution of the Ural–Mongol belt (UMB) and the amalgamation of Eurasia, we studied Middle Devonian basalts from two localities (11 sites) and Lower Silurian volcanics, redbeds, and intra-formational conglomerates from three localities (20 sites) in the Chingiz Range of East Kazakhstan. The Devonian rocks prove to be heavily overprinted in the late Paleozoic, and a high-temperature, presumably primary, southerly, and down component is isolated at only four sites from a homoclinal section. Most Silurian redbeds are found to be remagnetized in the late Paleozoic; in contrast, a bipolar near-horizontal remanence, isolated from Silurian volcanics, is most probably primary as indicated by positive tilt and conglomerate tests. Analysis of paleomagnetic data from the Chingiz Range shows that southward-pointing directions in Ordovician, Silurian, and Devonian rocks are of normal polarity and hence indicate large-scale rotations after the Middle Devonian. The Chingiz paleomagnetic directions can be compared with Paleozoic data from the North Tien Shan and with the horseshoe-shaped distribution of subduction-related volcanic complexes in Kazakhstan. Both paleomagnetic and geological data support the idea that today's strongly curved volcanic belts of Kazakhstan are an orocline, deformed mostly before mid-Permian time. Despite the determination of nearly a dozen new Paleozoic paleopoles in this study and other recent publications by our team, significant temporal and spatial gaps remain in our knowledge of the paleomagnetic directions during the middle and late Paleozoic. However, the paleomagnetic results from the Chingiz Range and the North Tien Shan indicate that these areas show generally coherent motions with Siberia and Baltica, respectively.

© 2003 Elsevier B.V. All rights reserved.

Keywords: East Kazakhstan; Middle Paleozoic; Oroclinal bending; Ural–Mongol fold belt; Paleomagnetism; Rotations

1. Introduction

Eurasia comprises several major blocks with Precambrian basement separated by mobile belts (figure I-1a; where the roman numeral I stands for figures that

[☆] Refers to doi:10.1016/j.tecto.2003.09.003.

* Corresponding author. Tel.: +1-734-764-8322; fax: +1-734-763-4690.

E-mail address: voo@umich.edu (R. Van der Voo).

are presented in the companion paper (Collins et al., 2003). The largest of these are the Alpine and Ural–Mongol belts which cover about half the Asian continent. While the former is the locus of Eurasia's growth during the Mesozoic and Cenozoic, the Ural–Mongol and Variscan belts played the same role throughout Paleozoic time. Tectonic evolution of the Alpine belt is relatively well understood because of three factors. First, we know the kinematics of the surrounding major plates from geological and geophysical data derived from the existing oceans. Second, motion of smaller tectonic units within the belt itself is constrained by numerous paleomagnetic data (Van der Voo, 1993). Third, many additional constraints are imposed on the Alpine belt evolution not only by paleolatitudes but also by rotations of tectonic units; classical examples include those that relate rotations of Sardinia and the Adria block to the evolution of the Western Mediterranean (e.g., Montigny et al., 1981; Channell et al., 1978).

The situation is much more vague for the Ural–Mongol belt (UMB), which stretches from the North Urals to Kazakhstan and Tien Shan and onward to Altai, Mongolia and the Pacific Coast (figure I-1a). This belt comprises many microcontinents with Precambrian crust and numerous island-arc domains separated by ophiolite sutures. The UMB separates the European, Siberian, North China, and Tarim cratons (figure I-1a); although we know something about the Paleozoic kinematics of these blocks from paleobiogeographic and paleomagnetic data, this knowledge is much less accurate than for the plates around the Alpine belt in the Mesozoic and Cenozoic. To date, only a few paleomagnetic results are available from within the UMB; still less can be considered reliable. Thus, most UMB tectonic units either have no paleolatitudinal readings altogether or, at best, have it for just one time. Clearly, the data scarcity and the complex, usually multistage, deformation of the UMB prevent elucidating the rotation pattern of these units. Consequently, a number of disparate tectonic models has been developed as summarized in the companion paper by Collins et al. (2003).

Kazakhstan is an area where the UMB reaches its maximum width and probably maximum complexity. As part of a program directed to paleomagnetic investigations of the UMB, we studied Paleozoic complexes, mostly of subduction-related volcanic

affinity, in the Chingiz Range of East Kazakhstan (figure I-1b). In the companion paper, new early Paleozoic data from the Chingiz Range are presented, and its paleolatitudinal drift over the entire Paleozoic is analyzed. Here, we present new middle Paleozoic data from East Kazakhstan and analyze the rotation patterns in the central UMB.

2. Geological setting and sampling

The Chingiz Range is a part of the Boshekul–Chingiz zone, which is one of the first-order tectonic units of Kazakhstan (figure I-1b). This zone comprises Cambrian to Lower Silurian volcanic series of island-arc affinity, sedimentary filling of deep-water basins, and accretionary complexes (for detail, see Collins et al., 2003). Lower Silurian volcanics and clastic sediments are thus the youngest formations in the Chingiz island-arc complex (Degtyarev, 1999).

A drastic change in geodynamic setting took place in the Late Silurian, as revealed by a major angular unconformity and widespread granite intrusions (Degtyarev and Ryazantsev, 1993). Since that time, an Andean-type volcanic belt that unconformably covers all older structures began developing in Kazakhstan (figure I-1b). This strongly curved belt includes thick piles of acid Lower Devonian and intermediate to mafic Middle Devonian volcanics. Marine sedimentation was preserved only in the inner part of the volcanic loop. The inner boundary of the belt is sharp but not marked by a continuous belt-bounding fault system. In contrast, the outer boundary of the belt is diffuse, and Devonian intrusions, volcanic piles, and tuffaceous sequences are common outside of the belt *sensu stricto*.

We studied the central part of the Chingiz zone near its southwestern margin and the adjacent part of the Devonian volcanic belt in two areas (Fig. 1). In the northern one (Fig. 1a), the youngest member of the island-arc series is a thick pile of andesitic to basaltic volcanics with redbed members. Different groups of fossils from sedimentary interbeds indicate a late Llandoveryan–Wenlockian age of this pile (Bandaleto, 1969), which conformably overlaps Lower Silurian terrigenous rocks, mostly sandstones, which in turn conformably rest on Upper Ordovician (Caradocian–Ashgillian) andesites with volcano-sedimentary

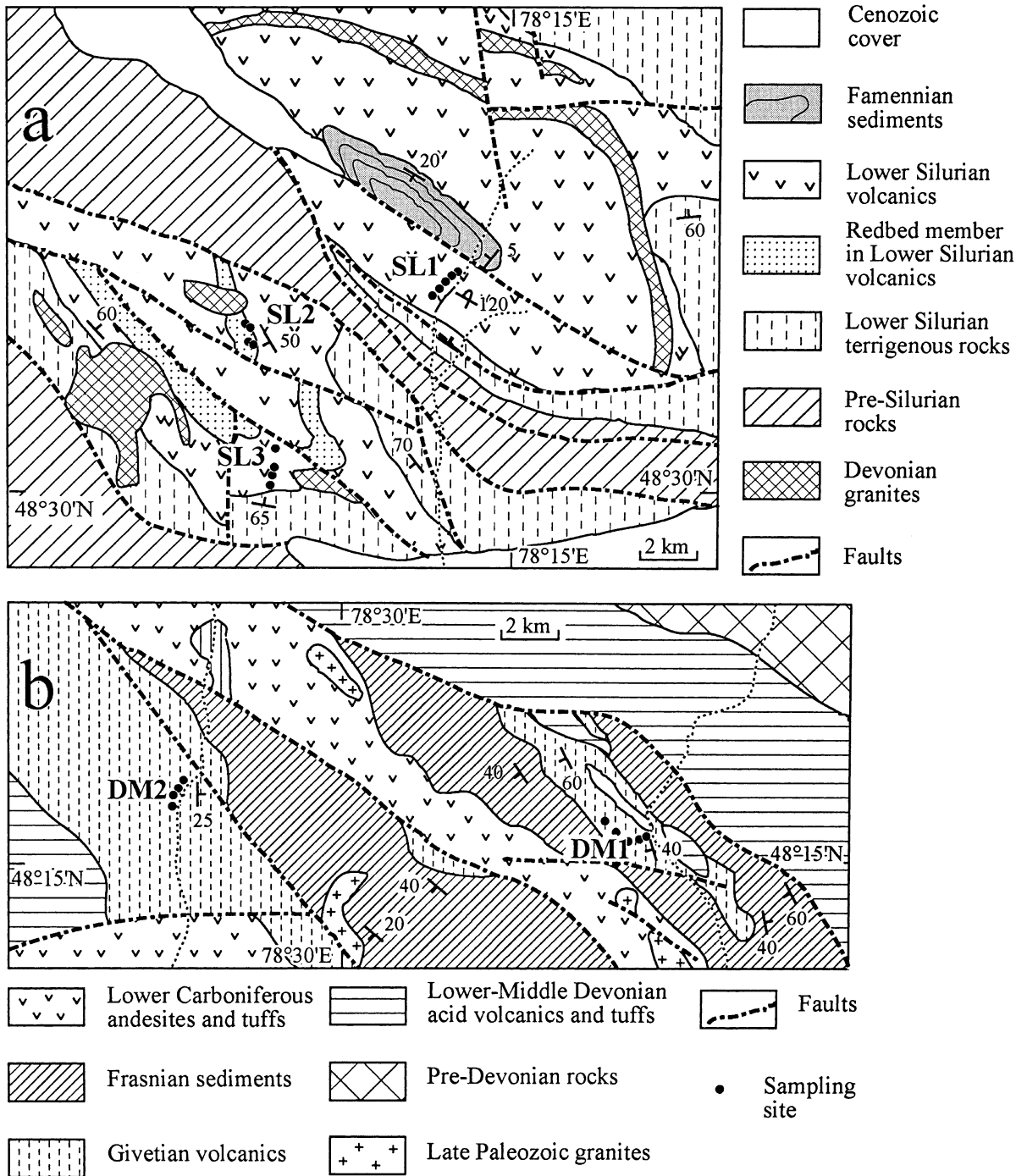


Fig. 1. Schematic geological maps of the Silurian (a) and Devonian (b) sampling localities labeled as in the text; for the overall locations of these sampling areas, see the overview maps presented as figure I-1 in Collins et al. (2003).

and limestone interbeds (Nikitin, 1972). No Lower–Middle Devonian formations are found in this northern area (Fig. 1a), and Famennian sediments unconformably cover all older rocks. This area is cut by NW–SE-trending faults with dextral strike–slip displacement of a few kilometers; these faults are most likely of late Paleozoic to early Mesozoic age.

Green rocks predominate among the Lower Silurian sedimentary sequence in the northern study area; field observations on a few red layers appear to indicate that they are the unleached remnants. In addition, these rocks are usually severely deformed with a well-developed cleavage. As a result, this sequence was found to be unsuitable for paleomagnetic sampling.

Lower Silurian volcanics proved to be a difficult paleomagnetic target as well. At many exposures, these rocks consist of either agglomerated lava or superbly looking basalt and andesite sequences without any stratification. Nevertheless, we found three localities (SL1–SL3, Fig. 1a) where bedding attitudes could be accurately determined from sedimentary intercalations. It is known that a fold test is rendered inconclusive when a shallow remanence direction is approximately parallel to the strike of bedding. Lacking a priori information about Silurian declinations, we sampled sections with at least three different strikes. NW–SE-trending structures are common in the area (Fig. 1a), but the only suitable sampling section with nearly N–S strike was found at SL2. At locality SL1, several dark-colored basalt and andesite-basalt flows (sites S1–S5, S7) and lava clasts from an intra-formatinal conglomerate (site S6) were sampled. Similar volcanics (sites S8–S10), lava clasts from an intra-formatinal conglomerate (site S11), and medium-grained red sandstones (sites S12–S16) were taken at locality SL2. Finally, similar volcanics and their tuffs were sampled at locality SL3 (sites S17–S20).

The southern area lies within the Devonian volcanic belt, which forms a nearly continuous band generally to the south and southwest from the Silurian volcanic belt (figure I-1b). A thick pile of acid Lower Devonian volcanics unconformably covers pre-Devonian rocks in this area. Without angular unconformity, Middle Devonian black basalts with sedimentary interbeds containing Givetian fossils overlie the acid volcanics and are in turn conformably overlain by

Frasnian sediments. Devonian rocks are covered by Lower Carboniferous andesites with angular unconformity.

The Middle Devonian basalts were studied at two separate localities (DM1 and DM2, Fig. 1b). Volcanics were sampled either directly above or below sedimentary units from which the bedding attitudes were determined. The only exception is in locality DM2 where only a single sedimentary layer was found, whereas the volcanics were sampled over an interval of section some 100 m thick, likely representing several eruptive events. Each site represents a few meters to several tens of meters of the section. In total, 180 samples of Lower Silurian rocks and 77 samples of Middle Devonian basalts were taken.

3. Methods

Six to fifteen hand samples, oriented with a magnetic compass, were taken at each site and cut into standard 8-cm³ specimens in the laboratory. Magnetic susceptibility of volcanics was measured in the field with the aid of a Czech portable kappameter KT5. One cubic specimen from each hand sample was subjected to progressive thermal demagnetization in 15–20 steps up to 690 °C. The specimens were thermally demagnetized in a homemade oven with internal residual fields of about 10 nT and measured with a JR-4 spinner magnetometer with a noise level of 0.1 mA/m. Demagnetization results were plotted on orthogonal vector diagrams (Zijderveld, 1967). Because of a strong drop of NRM intensity in many samples after heating to 200 °C, demagnetization data are presented without the initial step (e.g., Fig. 2). Linear trajectories were used to determine directions of magnetic components by a least-squares fit comprising three measurements or more (Kirschvink, 1980). The characteristic remanent magnetization, ChRM, was determined with or without anchoring the final linear segments to the origin of vector diagrams, depending on the case; dashed lines in the diagrams indicate the trajectories selected. Components isolated from the samples and/or remagnetization circles were used to calculate site means (McFadden and McElhinny, 1988). Paleomagnetic software written by Randy Enkin and Stanislav V.

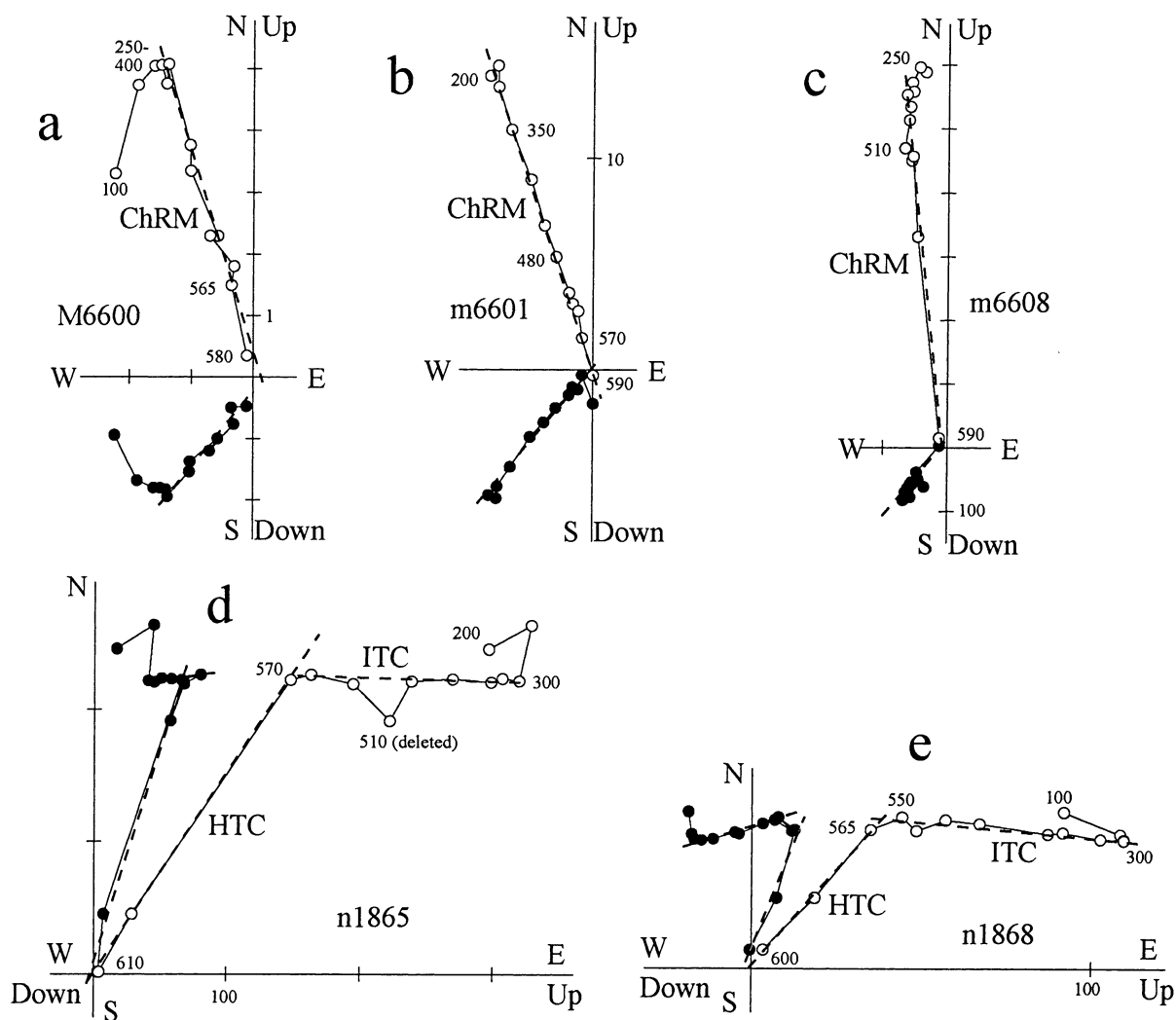


Fig. 2. Representative thermal demagnetization plots of Middle Devonian volcanics from the Chingiz Range in geographic coordinates. (a–c) Locality DM1; (d and e) locality DM2. Full (open) dots represent vector endpoints projected onto the horizontal (vertical) plane. Temperature steps are in degrees Celsius. Magnetization intensities are in milliamperes per meter. Thick dashed lines denote component trajectories as determined with principal component analysis and labeled as in the text. For clarity, NRM points are omitted from the plots.

Shipunov for the IBM PC and by Jean-Pascal Cogné for the Macintosh was used in the analysis.

4. Results

4.1. Middle Devonian rocks

Despite the visible freshness, most dark-gray to black basalts from locality DM1 have a susceptibility

less than 10^{-3} SI units as measured in the field. This is 10–100 times lower than typical basaltic values. The NRM of most basalt samples range from 1 to 10 mA/m, which is again lower than typical basalt remanence by a factor of 100. After removal of a low-temperature component, a single component was isolated between 300–350°C and 510–590°C from DM1 volcanics (Fig. 2a–c). The corresponding linear segments either slightly miss the origin (Fig. 2a and c) or decay to it (Fig. 2b). Site means are well

defined and are better grouped in situ than after tilt correction (Table 1); the best data grouping is in situ as observed in incremental unfolding. Hence, the volcanics from this locality are completely remagnetized after folding.

Both the NRMs and susceptibilities are about 10 times stronger at locality DM2. Intermediate- (ITC) and high (HTC)-temperature components were recognized in many samples (Fig. 2d and e). There is no tilt test for this locality because of homoclinal bedding (Table 1). When the ITC directions are combined with the data from locality DM1, the 11 site means are much better grouped in situ than after tilt correction (Table 1; Fig. 3a and b); the best data grouping is again achieved in situ, indicating a post-folding age of the ITC from locality DM2. At the same time, the data from locality DM1 and the HTC directions of DM2 better agree after tilt correction (Table 1). We think, however, that this agreement is fortuitous, as the tilt test is definitely negative for the DM1 data.

Although a Devonian age of the mean HTC direction of locality DM2 could not be confirmed by any field test, its reliability is (weakly) supported by rectilinear decay to the origin at the final steps of demagnetization (Fig. 2d and e) and by remoteness from both late Paleozoic overprint (Fig. 3c and d) and any expected post-Paleozoic field directions. We think that it is likely that the HTC from locality DM2 represents a Devonian remanence, but concede that it is rather poorly defined (Table 1).

4.2. Lower Silurian rocks

Some samples of Lower Silurian volcanics reveal no consistent directional pattern after heating to 200 °C. Other samples have very strong remanence (>10 A/m) and show superb linear trajectories until 560–580 °C, sometimes even at higher temperatures (not shown). This major component, however, is directionally random. Though relief highs were avoided, these strongly magnetized samples are likely to have been

Table 1
Paleomagnetic results from the Middle Devonian (Givetian) volcanics

| Site | N | In situ | | | | | Tilt corrected | | | |
|------------|---------|---------|-------|-------|-----|---------------|----------------|-------|-----|---------------|
| | | A | D (°) | I (°) | k | α_{95} | D (°) | I (°) | k | α_{95} |
| <i>ITC</i> | | | | | | | | | | |
| D1 | 7/7 | 194/40 | 230.2 | –63.1 | | | 331.7 | –66.6 | 70 | 7.3 |
| D2 | 8/8 | 216/37 | 235.0 | –74.4 | | | 22.9 | –67.2 | 132 | 4.8 |
| D3 | 7/7 | 216/37 | 232.8 | –74.8 | | | 24.8 | –67.2 | 131 | 5.3 |
| D4 | 7/6 | 225/61 | 238.9 | –71.3 | | | 38.5 | –47.0 | 54 | 9.2 |
| D5 | 8/6 | 220/65 | 255.3 | –66.5 | | | 21.6 | –43.1 | 46 | 10.0 |
| D6 | 6/6 | 242/41 | 260.3 | –62.2 | | | 31.4 | –73.7 | 75 | 7.8 |
| DM1 Mean | (6/6) | | 243.4 | –69.2 | 121 | 6.1 | 21.0 | –62.4 | 25 | 13.7 |
| D7 | 7/6 | 85/20 | 278.0 | –79.9 | | | 269.5 | –60.1 | 44 | 10.2 |
| D8 | 7/3 | 85/20 | 269.6 | –67.6 | | | 267.6 | –47.6 | 47 | 18.1 |
| D9 | 7/6 | 85/20 | 235.6 | –66.2 | | | 247.9 | –47.7 | 22 | 14.8 |
| D10 | 6/6 | 85/20 | 232.2 | –73.8 | | | 249.6 | –55.3 | 15 | 17.8 |
| D11 | 7/6 | 85/20 | 262.7 | –72.4 | | | 263.9 | –52.4 | 16 | 17.2 |
| DM2 mean | (5/5) | | 253.6 | –72.8 | | | 259.4 | –53.0 | 99 | 7.7 |
| ITC mean | (11/11) | | 247.6 | –70.9 | 110 | 4.4 | 314.9 | –73.0 | 7 | 19.0 |
| <i>HTC</i> | | | | | | | | | | |
| D7 | 7/4 | 85/20 | 0.7 | –43.8 | | | 341.0 | –44.4 | 12 | 27.1 |
| D8 | 7/6 | 85/20 | 6.0 | –53.1 | | | 338.3 | –54.3 | 53 | 9.9 |
| D9 | 7/7 | 85/20 | 18.1 | –40.5 | | | 359.7 | –47.4 | 63 | 7.9 |
| D11 | 7/5 | 85/20 | 26.2 | –38.3 | | | 9.5 | –48.1 | 217 | 5.4 |
| DM2-HTC | (5/4) | | 13.4 | –44.4 | 58 | 12.2 | 352.4 | –49.3 | 58 | 12.2 |

N is the ratio of the number of samples (sites) studied/accepted; A is the mean azimuth of dip/dip angle; D, declination; I, inclination; k, concentration parameter (Fisher, 1953); α_{95} , radius of confidence circle; ITC is the intermediate temperature component, and HTC is the high-temperature component; DM1 and DM2 are the two localities with six and five sites, respectively (for locations, see Fig. 1b).

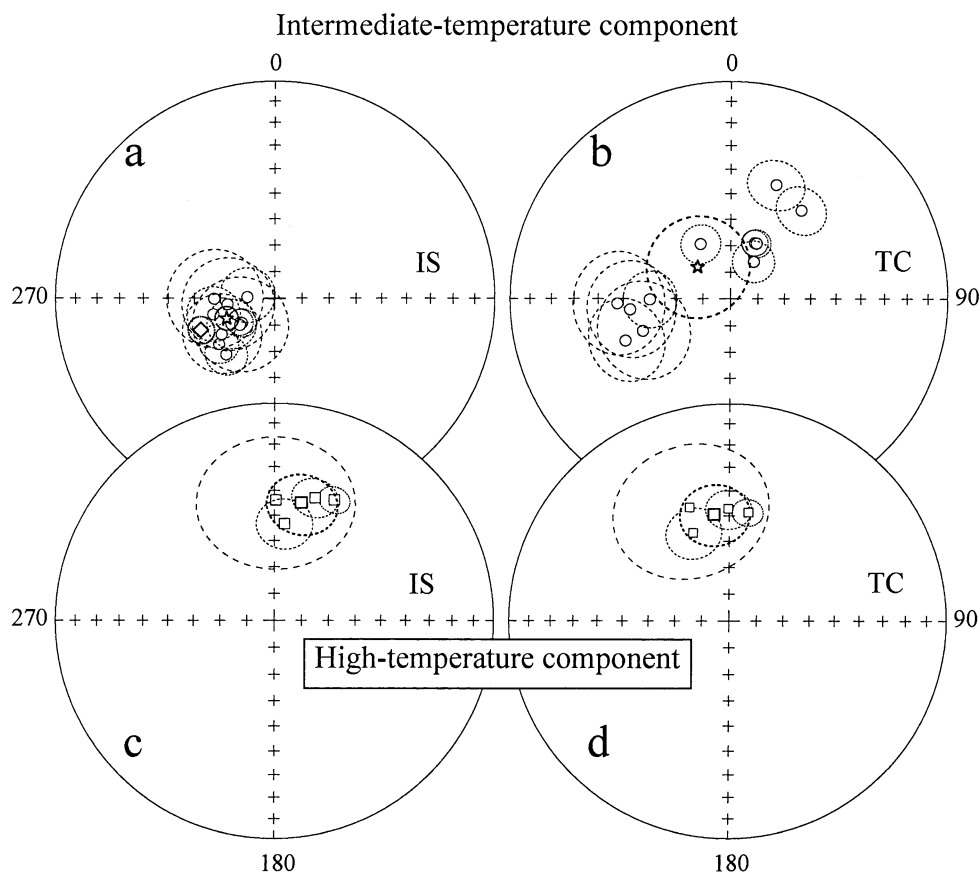


Fig. 3. (a and b) Stereoplots of ITC site-mean directions (circles) with confidence circles (thin dashed lines) in Middle Devonian volcanics from the Chingiz Range in situ (a) and after tilt correction (b). (c and d) HTC site-mean directions (squares) from bi-component samples from locality DM2 in situ (c) and tilt corrected (d). All (open) symbols are projected onto upper hemisphere. Stars are the overall mean directions of the ITC from localities DM1 and DM2 with their confidence circles (thick line); thicker squares are the overall HTC means with their confidence circles (thicker dashed line); large diamond in (a) is the Permian Eurasian reference direction with its confidence circle.

affected by lightning (e.g., Miller et al., 2000). Only after removal of 95–98% of the total remanence, do some samples start moving along great circles, which could be used for further analysis.

After excluding the lightning-affected part of the collection, some samples reveal a single component over the entire temperature interval, but the presence of two components is usually clear (Fig. 4a–d). An ITC may be removed from 350° to as high as 600°. This component is adequately grouped at two sites (Table 2) and random at the others (not listed in Table 2). Tentatively, this high scatter may be attributed to the sum of present-day components, late Paleozoic overprints, and relatively weak lightning effects.

The HTC shows rectilinear decay to the origin and can be easily isolated (Fig. 4a–d). If superposed components prevented proper isolation of this remanence, intersections of remagnetization circles identified above 450–500°C were used for calculation of site-mean directions. The HTC resides in magnetite (Fig. 4a) and/or hematite (Fig. 4b and c). In some samples, both minerals are its carriers (Fig. 4d), as suggested by the clear two-step structure of remanence vs. temperature plots (Fig. 4e).

After removal of a weak and highly dispersed low-temperature component, a component persisting from 300° to 600° or 650°C was identified in red sandstones from sites S13–S16 at locality SL2. This

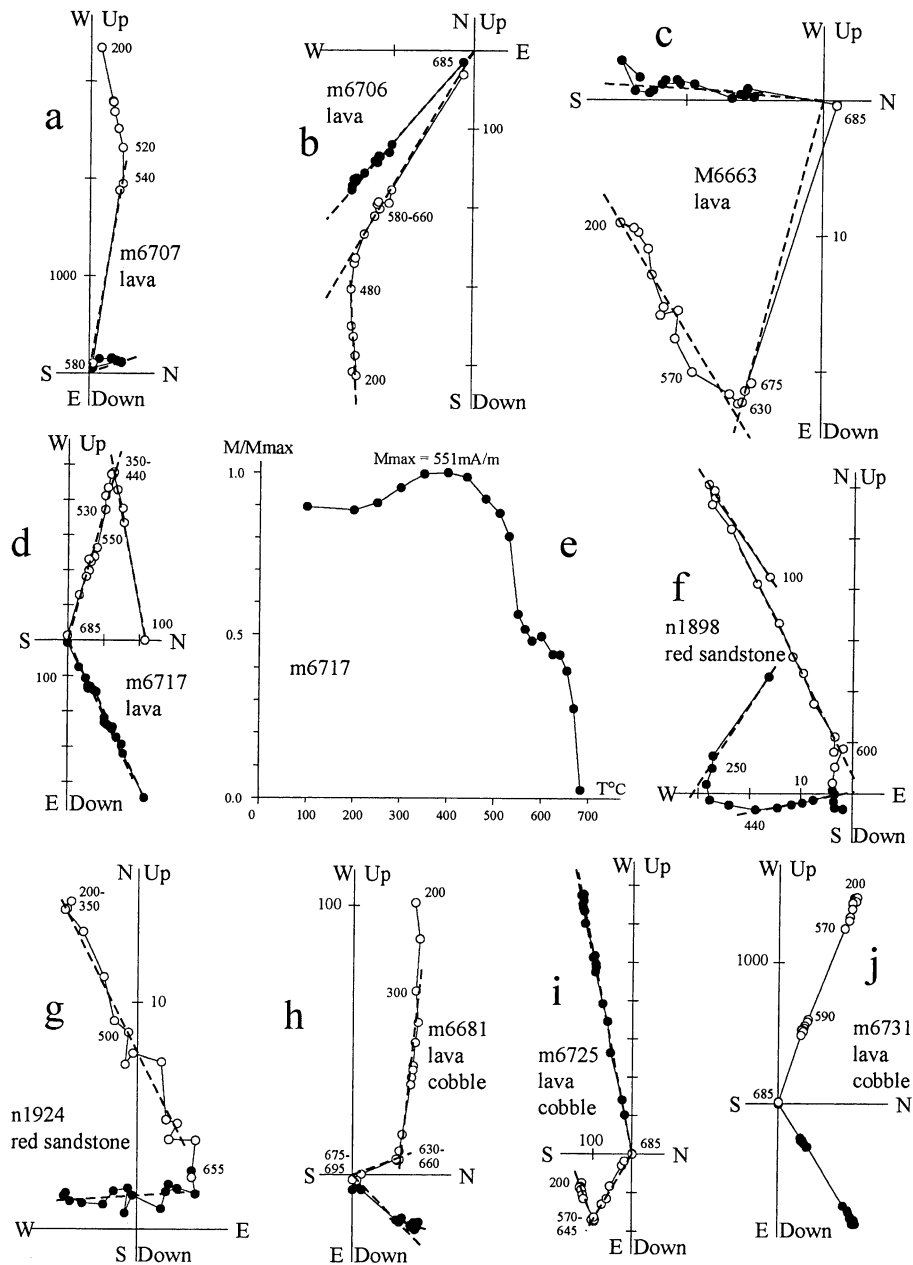


Fig. 4. Representative thermal demagnetization plots (a–d, f–j) and a plot of NRM intensity versus temperature (e) for Lower Silurian volcanics (a–e), redbeds (f and g) and clasts from intra-formational conglomerate units (h–j). Other notation as in Fig. 2.

component does not decay to the origin (Fig. 4f and g), and the presence of a HTC can be recognized, but it cannot properly be isolated because of acquisition of spurious remanences above 600°C.

Combining ITC data from redbeds with those from volcanics, it becomes clear that these directions are better grouped in situ than after tilt correction, except for the anomalous site S2 (Table 2; Fig. 5a and b). In

Table 2

Paleomagnetic results from Lower Silurian volcanics and redbeds of the Chingiz Range

| Site | N | In situ | | | | | Tilt corrected | | | |
|---|---------|---------|-------|-------|-----|---------------|----------------|-------|-----|---------------|
| | | A | D (°) | I (°) | k | α_{95} | D (°) | I (°) | k | α_{95} |
| <i>Intermediate-temperature component</i> | | | | | | | | | | |
| S1v | 6/4 | 66/116 | 217.8 | −67.4 | 24 | 19.0 | 231.1 | 45.1 | 24 | 19.0 |
| S2v* | 7/6 | 66/116 | 331.8 | −15.1 | 7 | 27.9 | 324.1 | 10.2 | 7 | 27.9 |
| S13r | 7/4 | 218/47 | 212.7 | −72.5 | 12 | 27.8 | 41.2 | −60.4 | 12 | 27.8 |
| S14r | 11/9 | 249/56 | 275.0 | −62.1 | 86 | 5.6 | 46.8 | −57.0 | 108 | 5.0 |
| S15r | 12/11 | 259/46 | 277.9 | −75.7 | 30 | 8.5 | 70.9 | −57.3 | 29 | 8.6 |
| S16r | 11/11 | 271/75 | 245.9 | −74.0 | 40 | 7.3 | 99.5 | −31.7 | 14 | 12.4 |
| Mean ITC | (18/5) | | 246.4 | −72.4 | 50 | 10.9 | 77.5 | −56.6 | <3 | 81.5 |
| S+D ITC | (16) | | 236.5 | −70.8 | 88 | 4.1 | 355.1 | −77.7 | 3 | 24.7 |
| <i>High-temperature component</i> | | | | | | | | | | |
| S2v | 7/5 | 66/116 | 273.3 | 45.5 | 54 | 10.9 | 46.6 | 14.3 | 54 | 10.9 |
| S4v | 9/9 | 21/120 | 353.7 | −62.2 | 8 | 20.0 | 213.4 | 4.8 | 8 | 20.0 |
| S5v | 9/8 | 24/88 | 171.2 | −80.2 | 13 | 16.4 | 198.3 | 5.8 | 14 | 16.1 |
| S7v | 8/7 | 26/127 | 64.0 | −64.5 | 15 | 16.4 | 189.6 | 16.0 | 17 | 15.3 |
| Mean SL1 | (6/4) | | 247.3 | 71.7 | 9 | 32.2 | 27.0 | −3.2 | 16 | 23.9 |
| S8v | 9/8 | 220/72 | 346.8 | −55.6 | 12 | 16.5 | 13.2 | 3.3 | 13 | 16.4 |
| S9v | 9/9 | 220/72 | 358.4 | −71.9 | 33 | 9.3 | 28.0 | −4.4 | 32 | 9.5 |
| S10v | 9/8 | 219/69 | 55.7 | −71.7 | 18 | 13.7 | 44.5 | −3.4 | 19 | 13.4 |
| S12r | 15/7 | 292/46 | 201.1 | −0.1 | 6 | 27.5 | 201.4 | 0.8 | 7 | 26.2 |
| Mean SL2 | (8/4) | | 13.7 | −53.3 | 5 | >45 | 26.7 | −1.4 | 35 | 15.7 |
| S17v | 6/5 | 32/59 | 285.3 | −71.9 | 67 | 9.4 | 231.1 | −24.4 | 67 | 9.4 |
| S18v | 8/8 | 32/59 | 236.8 | −49.9 | 10 | 18.6 | 227.8 | 6.2 | 10 | 18.6 |
| S19v | 6/6 | 28/56 | 293.8 | −71.2 | 134 | 5.8 | 230.0 | −30.6 | 134 | 5.8 |
| S20v | 13/9 | 28/74 | 287.7 | −38.9 | 14 | 14.7 | 258.6 | −1.5 | 13 | 15.1 |
| Mean SL3 | (4/4) | | 92.9 | 60.3 | 14 | 25.3 | 57.2 | 12.9 | 13 | 26.7 |
| Mean NE | (4) | | 330.8 | −58.7 | <3 | | 32.0 | 2.5 | 21 | 20.6 |
| Mean SW | (8) | | 259.3 | −72.6 | 4 | 30.5 | 218.4 | −2.9 | 9 | 19.7 |
| Mean all | (18/12) | | 222.1 | −64.5 | <3 | >45 | 216.5 | −2.8 | 12 | 13.3 |
| INCL only | (18/12) | | – | −55.7 | <3 | >45 | – | −2.7 | 15 | 8.2 |

Sites are labeled as in the text; characters v and r stand for volcanics and redbeds, respectively. S+D ITC is the overall mean of overprint data for the Silurian and Devonian rocks. NE, SW, means for vectors with northeastern and southwestern tilt-corrected declinations, respectively. The overall means (mean all, INCL only) are given as SW-pointing vectors. Other notation as in Table 1.

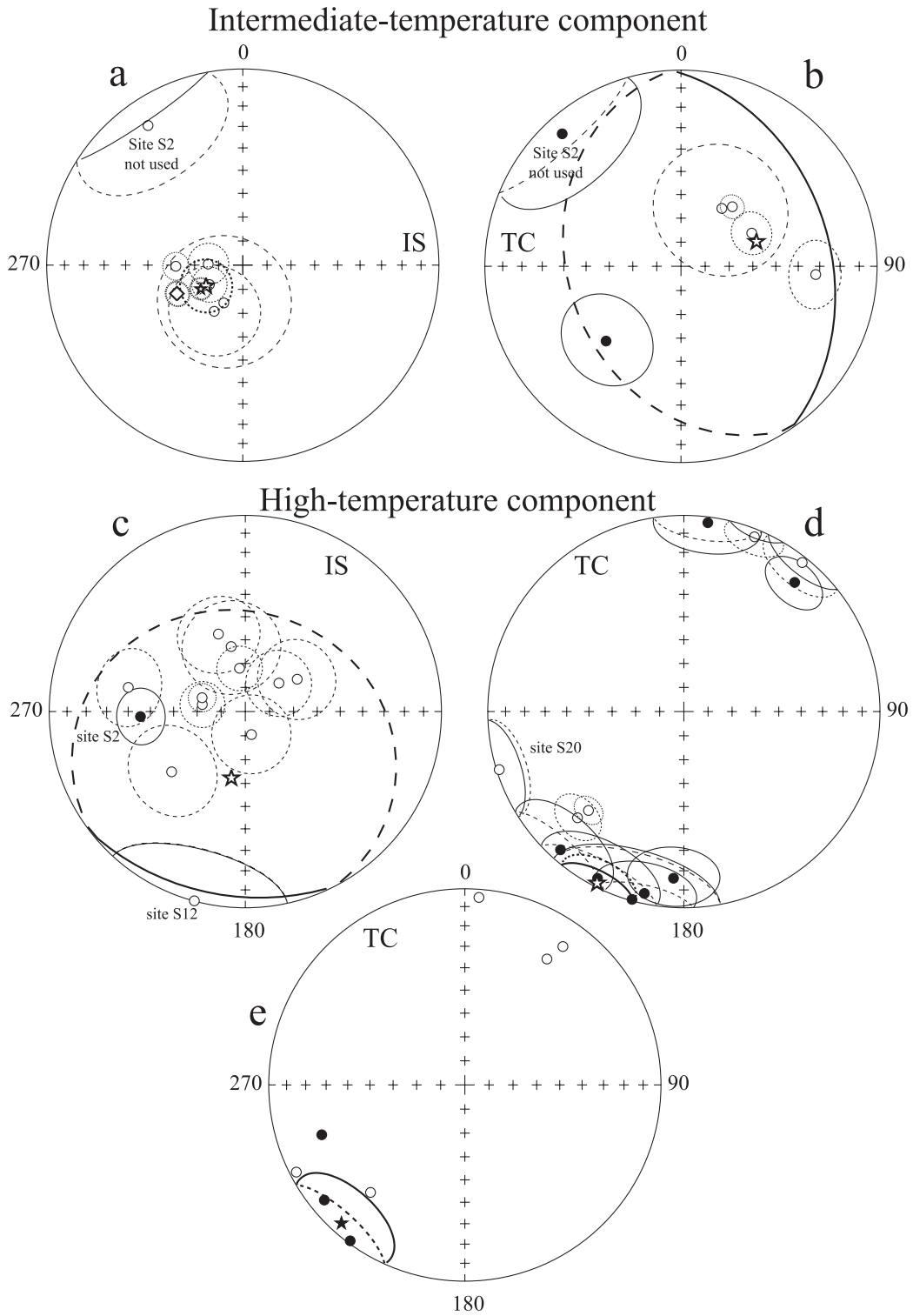
* Anomalous result; excluded from analysis.

contrast, no consistent ITC directions were found at site S12 about 1 km away, whereas adequately grouped HTC directions were isolated from seven samples at this redbed site. This pattern closely resembles that in volcanics; the tilt-corrected HTC mean for site S12 (Table 2) matches those of the volcanic HTC means.

The results from locality SL3 are all from volcanics and comprise only HTC directions, which have—after tilt correction—shallow inclinations similar to those of the other two localities. The declinations after tilt correction are somewhat more westerly, notably so for site S20 (Table 2; Fig. 5d). This pattern can be

attributed to local rotations, which are likely in this area dissected by strike–slip faults (Fig. 1a).

After tilt correction, the HTC site means from all three localities fall into two nearly antipodal groups, which most likely represent two polarities (Fig. 5d). The polarity means differ by 174°, but because of the dispersed declinations their cones of 95% confidence are large (Table 2) and the reversal test is indeterminate (McFadden and McElhinny, 1990). Grouping of site means in each polarity group improves after tilt correction (Table 2: Mean NE, Mean SW). For the combined set of 12 site means, the best grouping of data is achieved at 100% unfolding.



Because of the more westerly declinations of locality SL3, we have also used an inclination-only tilt test and its statistics (McFadden and Reid, 1982); for the set of 12 site means, the inclination-only tilt test is positive, and the best grouping of data is achieved at 100% unfolding. Hence, the dual-polarity ChRM in Lower Silurian rocks appears to have been acquired prior to all subsequent folding events in this area, the oldest of which took place in the Late Silurian.

What still needs to be addressed, however, is the scattered grouping of 10 site means out of 12 before tilt correction on the upper hemisphere, because this is not very far away from the late Paleozoic overprint (Fig. 5a). Such a pattern could be diagnostic of post-folding directions. Moreover, such a grouping will produce dual-polarity paleomagnetic directions when two limbs of an isoclinal fold are used, while the fold axis is approximately orthogonal to paleomagnetic vectors. The directions after tilt correction would then reveal a normal polarity in one limb and reversed polarity in the other limb. Because this unfavorable situation resembles our case for 10 of the 12 sites, the remaining 2 sites (S2 and S12) are of crucial importance. Site 2 comes from locality SL1 where other sites are of opposite polarity, whereas site 12 is from an outcrop with a bedding attitude that is different from those at other exposures. It is clear that sites S2 and S12 deviate from the others in situ and converge only after tilt correction (Fig. 5c and d). Note also that mean directions are given in Table 2 for that polarity that predominates at a given site. However, nearly antipodal directions are found within several sites, including sites S17–20 with the more westerly declinations (Fig. 5e). The fact that several sites internally have dual polarity directions negates the fear that the isoclinal fold setting artificially produces normal and reversed directions upon tilt correction.

The NRM of lava clasts at site S6 (9 clasts out of 12 studied) is dominated by an ITC, which may persist up to 630°; after its removal, an HTC is isolated from most samples (Fig. 4h). The ITC is

either much weaker or absent altogether at site S11, and a well-defined HTC is easily isolated (Fig. 4i and j). HTC directions are very dispersed but not completely random at site S6 (Fig. 6a and b); similarly, ITC vectors are dispersed but not random at this site (not shown). In contrast, HTC directions in 12 clasts out of 13 studied are randomly distributed at conglomeratic site S11 (Fig. 6c and d), where the normalized vector-resultant of 0.16 is less than the critical value of 0.46 of the Rayleigh test (Mardia, 1972).

Lava clasts at site S6 are immersed in a tuffaceous matrix and are overlain as well as underlain by lava flows. In contrast, clasts of similar volcanics were taken from a conglomerate unit surrounded by red sandstones at site S11. We assume that the conglomerate of site S6 was hot at the moment of accumulation and is actually an agglomerated lava flow, thus accounting for the fact that the scatter of HTC and ITC directions at this site is much larger than for adjacent host rocks; it is also possible that this conglomerate was partially remagnetized by overlying lava flows. These inferences can account for the fact that the direction of the vector resultant for the HTC at site S6 broadly agrees with the HTC mean direction of the host rocks after tilt correction. Very important is also the fact that the in situ mean HTC direction of site 6 is clearly different from the post-folding overprints in this area, which are steeply upward with southwestern declinations (Tables 1 and 2).

The HTC at site S11 resides in both magnetite and hematite (Fig. 4j), as is also found for host rocks at this locality (Fig. 4d and e); this indicates that oxidation of volcanics and hematite formation predated conglomerate accumulation. Although we are uncertain about possible explanations for the highly dispersed but still nonrandom distribution of HTC data at site S6, the evidence that acquisition of the HTC in site 11 predated accumulation of intra-formational conglomerate units convinces us that the remanence in these volcanics is primary.

Thus, the positive tilt test, the presence of two polarities, and the positive conglomerate test of site

Fig. 5. (a and b) Stereoplots of site-mean directions (circles, dots) with confidence circles (thin lines) of the ITC (a and b) and HTC (c and d) from Lower Silurian rocks in situ (a and c) and after tilt correction (b and d). Solid (open) symbols and solid (dashed) lines are projected onto lower (upper) hemisphere. Stars are the overall mean directions with their confidence circles (thicker lines). (e) HTC sample directions from site S18, after tilt correction, showing dual polarity. Other notation as in Fig. 3.

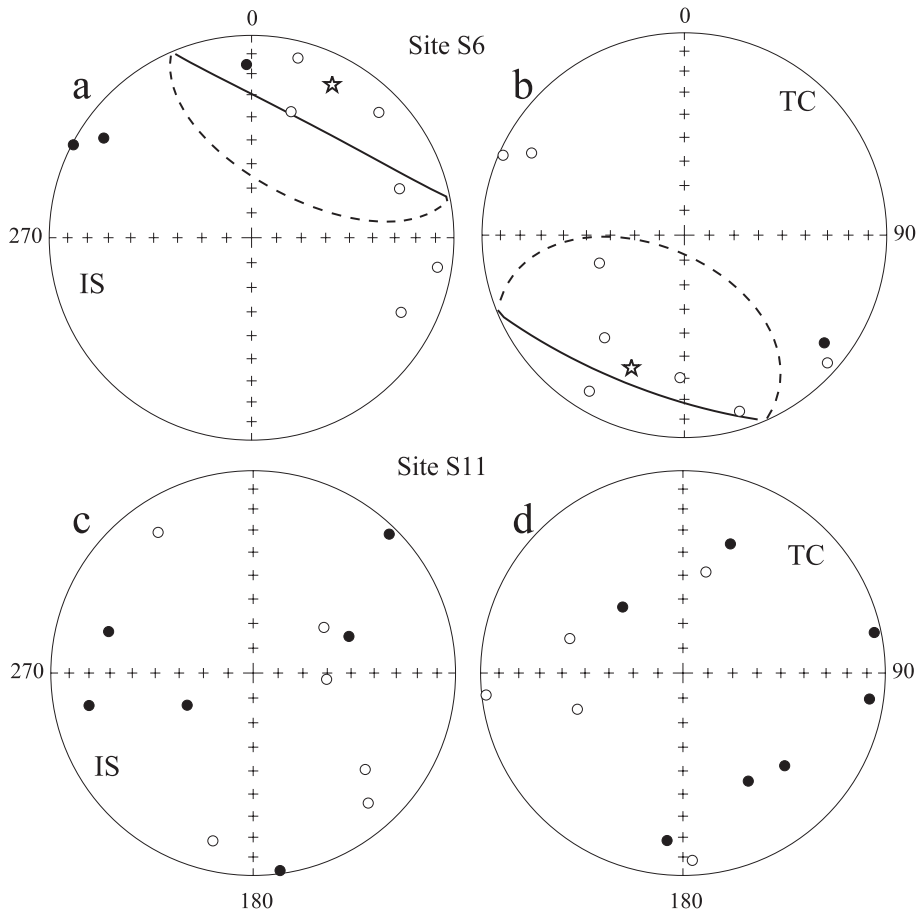


Fig. 6. (a and b) Stereoplots of HTC directions from clasts in intra-formational conglomerates from site S6 (a and b) and site S11 (c and d) in situ (a and c) and after tilt correction (b and d). Solid (open) symbols and solid (dashed) lines are projected onto lower (upper) hemisphere. Stars are the overall mean directions with their confidence circles (thicker lines) for the nonrandom data sets of site S6 (see text). Other notation as in Fig. 3.

S11 collectively indicate that the remanence in these rocks is Early Silurian in age. The mean inclination of $2.7 \pm 8.2^\circ$ indicates that the Chingiz Range was at an equatorial latitude of $1.4 \pm 4.1^\circ$ in the Early Silurian.

4.3. Overprint data

Good agreement of post-folding overprint directions in both Middle Devonian (Table 1) and Lower Silurian rocks (Table 2) makes it reasonable to combine them and calculate the overall mean (entry S+D ITC, Table 2), which has a steep mean inclination of $-70.8 \pm 4.1^\circ$. This value is steeper upward than the expected Permian ones of about -50° or even the Early Triassic one of -64° recalculated for the study

area from the apparent polar wander paths (APWP) for Baltica and Siberia (e.g., Van der Voo, 1993) but resembles younger Middle–Late Triassic reference directions.

There are rather sparse Lower Triassic volcanics in East Kazakhstan (Bekzhanov et al., 2000), which may be connected with remagnetization. A steep inclination of about 70° in these volcanics (Lyons et al., 2002) apparently confirms this possibility. Note, however, that all the overprint directions we found are reversed and so are the post-folding overprints in the northern part of the Chingiz Range (Collins et al., 2003) and other parts of East Kazakhstan (Grishin et al., 1997; Didenko and Morozov, 1999). Therefore, the remagnetization in Kazakhstan was almost defi-

nately of regional extent, thus rendering such an event unlikely in the Triassic with its high reversal frequency (Opdyke and Channell, 1996).

If we assume a Permian age for the overprint, a higher-than-expected inclination may be accounted for by post-Permian southward motion of East Kazakhstan with respect to both Baltica and Siberia. The along-meridian component of this motion, however, must be of the order of 2000 km. Geological evidence for this is entirely lacking; moreover, this hypothetical displacement is not supported by Permian data from eastern Kazakhstan, which show minor, if any, northward drift of the area during post-Permian time (Levashova et al., 2003).

Any post-folding overprint data lack precise paleohorizontal control, and post-remagnetization tilts may displace the overprint vectors. Minor deformation did take place in eastern Kazakhstan both in the Mesozoic and Cenozoic, as revealed by folding of Jurassic rocks and neotectonic motion along some faults. In the study area, however, the lack of geological evidence, specifically the absence of post-Paleozoic rocks, precludes an assessment of any tilting.

What is important for interpretation of inclination data and hence paleolatitudes is usually of minor significance for declination data. Whatever the origin of the oversteep post-folding inclination, this does not much affect the overall mean declination, which remains southwesterly and thus closely resembles the Eurasian Permian to Triassic reference directions in the Chingiz Range.

5. Polarity options and consequences for rotations

For the paleolatitudinal motion of the Chingiz Range (Collins et al., 2003), the preferred northward drift scenario leads to normal polarity as the choice for both Late Cambrian and Early Ordovician data, while the polarity of the Silurian result played no role, as this direction is nearly horizontal (Table 2). However, if we want to address the rotational history of this area throughout the Paleozoic, a polarity choice for the Silurian data becomes quite important. First of all, we should note that the late Paleozoic–early Mesozoic overprint and the Middle Devonian HTC directions from the Chingiz Range (Table 1) almost certainly imply a northern hemisphere location, as the southern

hemisphere leads to insurmountable problems for the tectonic evolution of Kazakhstan; hence, a normal polarity Devonian direction should be downward. Thus, our upward inclinations in the Devonian sites are of reversed polarity. In turn, this means that a southerly declination represents a normal polarity. The roughly southward-pointing Silurian declination (216°) is, by the same reasoning, also of normal polarity. The Silurian and Early Ordovician declinations, 216° and 146° (Collins et al., 2003), respectively, imply a ca. 70° clockwise rotation during the Early Ordovician–Early Silurian interval, and a counterclockwise rotation of less than 45° during the Early Silurian–Middle Devonian interval. The opposite choice of polarity for the Silurian result would require much larger back-and-forth rotations of 110° and 135° , respectively, which seems less likely to us.

The normal-polarity declinations deduced by the above reasoning for the Chingiz area are shown in Fig. 7a and, at first glance, appear to show an unusual complexity of rotational movements. However, such rotations are not surprising for a relatively small tectonic unit like the Chingiz Range, which evolved from an island arc to an Andean-type margin, followed by amalgamation into a complex continental element during the mid- and late Paleozoic. Palinspastic maps depicting the Kipchak Arc model of Sengör and Natal'in (1996) are detailed enough (figure I-7b in Collins et al., 2003) to estimate rotations of the Chingiz unit and compare them with the observed directions (Fig. 7a and b). The comparison is, in our opinion, quite favorable. The largest discrepancy is for the Silurian declination, as it was also for Silurian paleolatitudes (Collins et al., 2003); these misfits are attributed to the low quality of the Silurian paleomagnetic data for Siberia that were used to position the Kipchak Arc. Even with the Silurian anomaly, the overall fit of the expected and predicted directions is much better than we had anticipated. We note in passing that the model of Didenko et al. (1994) does not predict any large declination changes for the Chingiz Range in the early Paleozoic and the Silurian.

The North Tien Shan (NTS) tectonic zone is placed far away from the Chingiz segment in the Kipchak Arc (figure I-7), and we applied the same approach to paleomagnetic directions from the NTS (Fig. 7c) obtained by Bazhenov et al. (2003). This approach

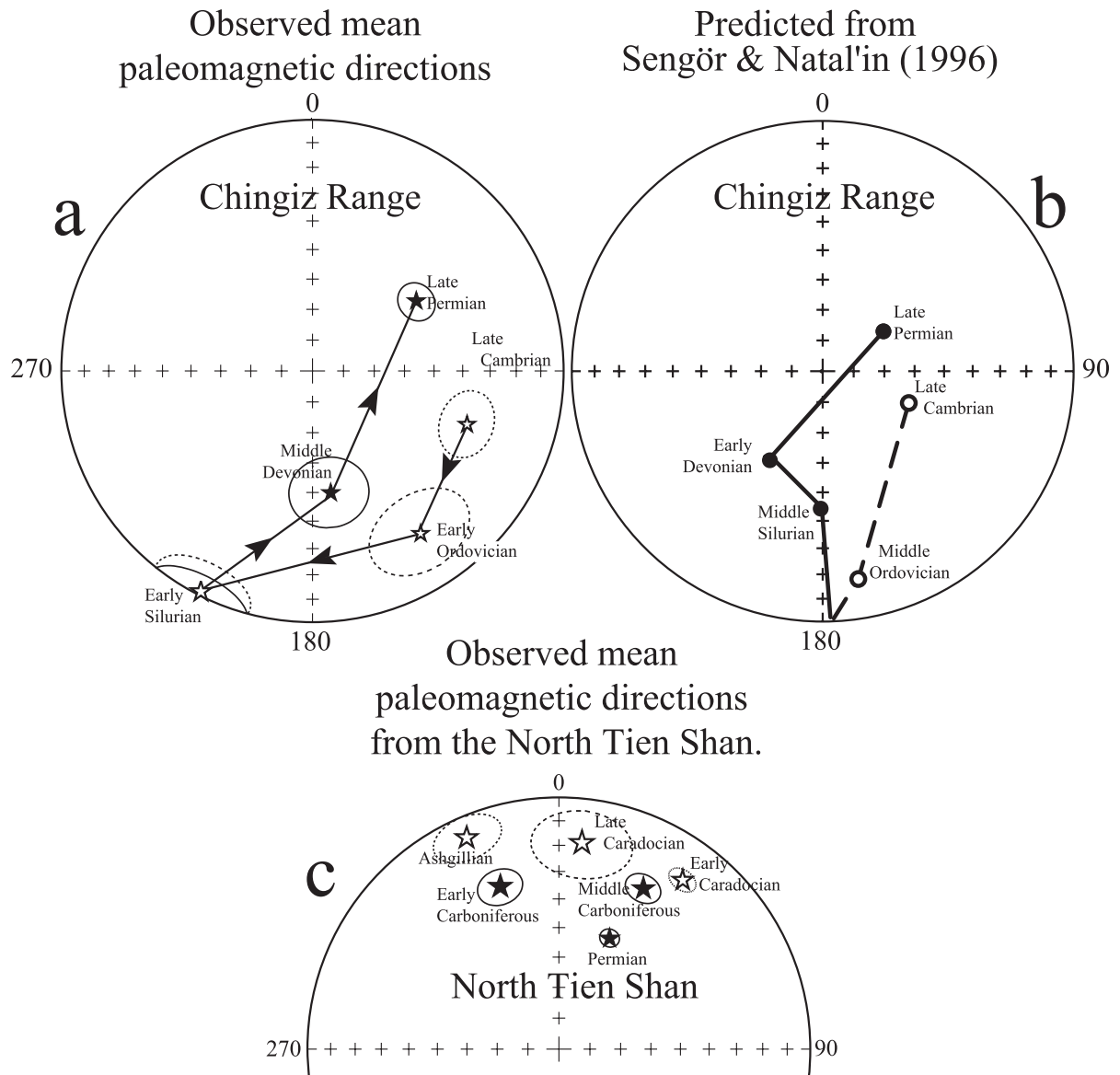


Fig. 7. Mean observed (a) and predicted (b) paleomagnetic directions for the Chingiz Range and observed directions (stars) from the North Tien Shan (c) shown with associated confidence circles. Solid (open) symbols and solid (dashed) lines are projected onto lower (upper) hemisphere. Other notation as in Fig. 3.

is much less successful, but undoubtedly, this is because we do not yet have a good regional and temporal paleomagnetic coverage, so that some local and regional rotations may thus far remain undetected. The NTS declinations are northerly, whereas the inclinations reveal a general northward drift as deduced from the change from low negative inclinations

in the Late Ordovician to moderate positive ones in the Early–Middle Carboniferous. Elongated declination distributions are characteristic of many results, suggesting rotations, not only within but also between localities—e.g., the 60° declination difference between Early and Middle Carboniferous (Fig. 7c). It is well known that the North Tien Shan suffered

strong internal dislocations, including rotations on a local to regional scale. Only when the spatial and temporal patterns of such rotations have been unraveled can we begin to have confidence in a comparison between observations and predictions from the *Sengör and Natal'in (1996)* model. At the present time, results from the NTS show evidence for some localized post-Permian rotations, whereas for pre-Permian time there are some rotations (see *Fig. 7c*) but they are not as large as the ca. 90° CW required by the Kipchak Arc model for the interval from the Middle Ordovician to the Permian.

6. Evidence for a large orocline in Kazakhstan

Volcanic activity progressively migrated inward across Kazakhstan's curved belts during the Late Devonian to Early Permian interval (*Fig. 8*). The last manifestations of volcanic activity consist of Upper Permian alkali mafic lava and Permian granite intrusions. In the late Paleozoic to early Mesozoic, eastern Kazakhstan was dissected by a set of NW–SE dextral strike–slip faults, with a subordinate vertical component of displacement in some places. The largest of them is the Chingiz Fault, which displaces Permian complexes by about 100 km (*Samygin, 1974*). Sparse Early Triassic volcanic activity in East Kazakhstan is related to extension associated with these strike–slip events (*Allen et al., 1995*).

While the middle–late Paleozoic tectonic pattern of Kazakhstan is dominated by a larger Early–Middle Devonian and a smaller late Paleozoic loop-like volcanic belt (*Fig. 8*), the early Paleozoic tectonic structure of Kazakhstan, as already noted, is very complicated, and the term “mosaic” has often been used to describe it. A recent analysis, however, showed that Cambrian and Ordovician volcanic complexes of island-arc affinity by and large follow the same loop-like pattern (*Degtyarev, 2003*). Generally, these complexes occupy external positions with respect to the younger volcanic belts, which also comprise mostly subduction-related volcanics (*Kurchavov, 1994; Kurchavov et al., 1999*). Hence, the continuous existence of a convergent boundary for more than 200 million years is strongly indicated. However, it is difficult to imagine a subduction zone of three-quarter circular form that was active along its entire length

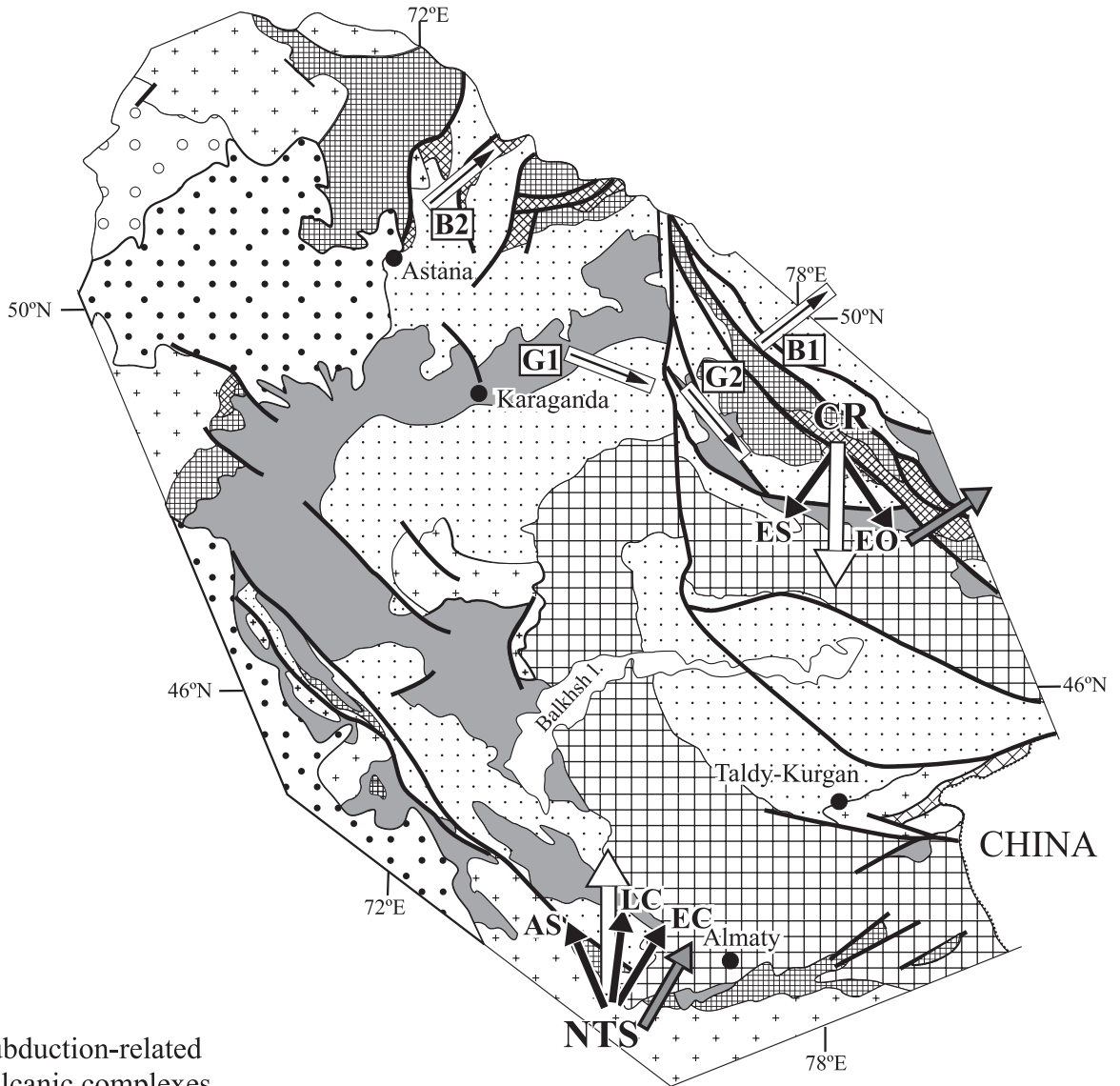
over such a long interval; instead, late Paleozoic bending of the loop is suggested.

The Early Ordovician and Early Silurian mean paleomagnetic directions from the Chingiz Range generally point southward, while the Late Ordovician data from the North Tien Shan point to the north (*Table 3*). This is premised on the assumption that all these vectors are correctly interpreted as being of normal polarity. If so, the difference in declinations of about 180° closely matches that in general strike of tectonic units at the opposite arms of the Kazakhstan loop. It appears that, notwithstanding all ambiguities, paleomagnetic data indicate complete oroclinal bending of Kazakhstan structures.

Although of limited reliability, our Middle Devonian direction from the Chingiz Range also points southward and implies that the orocline formation took place later. On the other hand, Late Permian primary directions and presumably Permian overprints from the Chingiz Range, as well as from the North Tien Shan, generally agree with Eurasian expected declinations (*Fig. 8*). Hence, the oroclinal bending has had to take place in the interval between the Middle Devonian and the Permian, but the lack of paleomagnetic data prevents more accurate dating of this large-scale tectonic event, which is clearly of first-order importance for the UMB evolution.


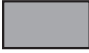
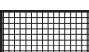

The paleomagnetism of Lower–Middle Devonian rocks, mostly volcanics, has also been studied at several other localities from two areas within, or close to, the Devonian belt (*Grishin et al., 1997*). Area-mean directions point to the southeast, indicating large rotations (G1 and G2, *Fig. 8*); indeed, the authors of this study interpreted the difference between these area means as indicating oroclinal rotations. The HTC directions in these rocks, however, form broad diffuse bands, which include the late Paleozoic expected direction; the unit vectors that were close to an expected remagnetization direction were excluded, and the remaining ones were treated as a primary Devonian remanence (*Grishin et al., 1997*).

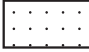

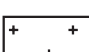

Burtman et al. (1998) reported paleomagnetic results from Middle Devonian volcanics and sediments from two other areas: one is close to the belt, while the other is clearly outside (B1 and B2, *Fig. 8*). The tilt and reversal tests for high-temperature components in these rocks are positive, but the mean



CHINA

Subduction-related volcanic complexes

-  Late Paleozoic
-  Early-Middle Devonian
-  Ordovician
-  Cambrian

-  Accretionary complexes of different ages
-  Ordovician back-arc complexes
-  Precambrian rocks
-  Late Paleozoic basins


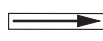


-  Permian declinations
-  Devonian declinations (published data)
-  Ordovician-Silurian declinations
-  Generalized Ordovician-Silurian declinations

Table 3
Summary of paleomagnetic results from the Chingiz Range and the North Tien Shan

| Directions | | | | | | | Poles | | |
|------------------------|----------|---------|---------|-----|-------------------|-----------|---------|---------|--------------|
| Result | Age (Ma) | D (°) | I (°) | k | α_{95} (°) | Plat (°) | F (°) | L (°) | A_{95} (°) |
| <i>Chingiz Range</i> | | | | | | | | | |
| MD | 377 ± 3 | 172.4 | 49.3 | 58 | 12.2 | 30 ± 11N | – 11.3 | 85.1 | 13.2 |
| ES | 426 ± 5 | – | – 2.7 | 15 | 8.2 | 1 ± 4S | – 33.6 | 32.7 | 9.4 |
| EO | 483 ± 5 | – | – 21.3 | 29 | 6.3 | 12 ± 4S | – 43.9 | 127.8 | 11.5 |
| LC | 515 ± 10 | 109.1 | – 35.2 | 33 | 9.8 | 19 ± 6S | – 27.0 | 168.2 | 8.6 |
| <i>North Tien Shan</i> | | | | | | | | | |
| P | 260 ± 7 | – | 49.7 | 51 | 2.6 | 30.5 ± 2N | 73.6 | 200.8 | 4.2 |
| B | 314 ± 6 | 27.6 | 28.3 | 100 | 5.2 | 15 ± 3N | 53.8 | 202.1 | 4.2 |
| VS | 326 ± 3 | 344.1 | 31.2 | 39 | 6.4 | 16 ± 2N | 61.6 | 287.2 | 5.4 |
| AS | 443 ± 5 | 336.6 | – 11.1 | 48 | 8.8 | 6 ± 5S | 37.4 | 281.1 | 6.3 |
| LC | 450 ± 3 | – | – 16.7 | 48 | 5.0 | 9 ± 3S | 38.2 | 246.5 | 9.0 |
| EC | 456 ± 3 | 31.1 | – 17.7 | 110 | 4.0 | 9 ± 3S | 31.1 | 214.7 | 2.9 |

For the Chingiz Range, MD, ES, EO, and LC are HTC in the rocks of Middle Devonian, Early Silurian, Early Ordovician, and Late Cambrian age, respectively (from this study and Collins et al., 2003). For the North Tien Shan, P is overall mean of Permian overprints; B, VS, AS, LC, and EC are HTC in Bashkirian, Viséan–Serpukhovian, Ashgillian, Upper Caradocian, and Lower Caradocian rocks, respectively (Bazhenov et al., 2003). Ages are assigned according to the DNAG time scale (after Palmer, 1983). All data are presented as normal polarity directions. For strongly elongated data sets (ES, EO, P, LC), mean inclinations and statistical parameters were calculated after McFadden and Reid (1982), in order to present the best estimate of the area's paleolatitude (Plat). Overall means for the same data sets were also calculated using Fisher (1953) and were used to compute pole positions (in italics); these poles would give paleolatitudes slightly different from those listed as calculated from inclination-only data. F , L , and A_{95} are the latitude, longitude, and radius of 95% confidence circle of the paleopole, respectively.

directions (B1: $D=52^\circ$; $I=41^\circ$, $A_{95}=6.4^\circ$, $N=40$ samples; B2: $D=50^\circ$; $I=31^\circ$, $A_{95}=8.9^\circ$, $N=18$ samples) are considerably different from the other Early–Middle Devonian results mentioned above. The Devonian rocks in these areas are thought to have been folded in Middle Carboniferous–Early Permian time (Burtman et al., 1998). The B1 and B2 mean directions agree both in declination and inclination with the late Paleozoic reference data for Baltica; against a late Paleozoic remagnetization, however, speaks the presence of both polarities. Also disturbing is the complete lack of late Paleozoic components in the B1 and B2 results (judging by the orthogonal plots presented), which heavily and often completely overprint all other Devonian rocks investigated in East Kazakhstan (Grishin et al., 1997; Didenko and Morozov, 1999; this paper). At the same time, the above reasons are not compelling, and the

results of Burtman et al. (1998) may prove to be of Devonian age and hence further complicate ideas about the tectonic evolution of Kazakhstan.

We admit that our interpretation of both latitudinal and rotational patterns of the Kazakhstan units is based on imperfect data and relies on additional assumptions. Elongated distributions of Early Ordovician and Early Silurian directions from the Chingiz and Late Caradocian directions from the North Tien Shan have been observed, and one can doubt the validity of computing mean declinations for such girdled distributions. Lacking adequate spatial coverage, each mean declination might have been affected by rotations on local scale; combining declinations of different ages is questionable as well. Last but not least, our interpretation heavily relies on the preferred polarity option. We cannot unambiguously counter these objections with the available data

Fig. 8. Schematic map of major rock complexes in East Kazakhstan (simplified after Degtyarev (2003)) and observed paleomagnetic directions labeled as in Table 3 from the Chingiz Range (CR) and the North Tien Shan (NTS) (see text for more details). Also shown are Devonian directions obtained in other studies: G1, G2, from Grishin et al. (1997); B1, B2, from Burtman et al. (1998).

Table 4

Summary of polarity options and geodynamic consequences for paleomagnetic data from the North Tien Shan and the Chingiz Range

| Polarity options | (1) All normal | (2) All reversed | (3) CR reversed NTS normal | (4) CR normal NTS reversed |
|-----------------------|----------------------------|----------------------------|-------------------------------|-------------------------------|
| Chingiz Range (CR) | ↓ | ↑ | ↑ | ↓ |
| North Tien Shan (NTS) | ↑ | ↓ | ↑ | ↓ |
| Latitudinal motion | general northward drift | general southward drift | CR southward NTS northward | CR northward NTS southward |
| Orocline | yes | yes | no | no |

Arrows indicate the declinations that normal polarity directions would have, if the polarity of the observed data is as listed in the column headings.

and indestructible reasoning. However, we can further support our interpretation with arguments based on simplicity, invoking Occam's razor. Table 4 summarizes the matrix of possibilities resulting from all possible polarity options. The preferred normal polarity interpretation of southward-pointing Chingiz and northward pointing North Tien Shan directions (option 1) creates a simple pattern of northward latitudinal movements and geologically sensible rotational movements. Option 2 is compatible with oroclinal bending but has Kazakhstan elements moving southward, which is in the opposite direction with respect to the general framework of the major cratons of Baltica and Siberia. The last two options (3 and 4) simply complicate the latitudinal movements such that each UMB unit incoherently moved by itself.

For the near future, our goal is to increase the paleomagnetic coverage both spatially and temporally, in attempts to substantiate the oroclinal bending model. Of considerable interest, albeit not presently possible, will be an attempt to explain the Paleozoic oroclinal bending of the Kipchak Arc in terms of geodynamics. However, unknown and unknowable paleolongitudes will hamper such efforts. While the paleolatitudinal positions of Baltica, Siberia, Tarim, and the North China Block are reasonably well understood, their relative east–west positions have remained speculative.

7. Conclusions

Thermal demagnetization reveals a high-temperature component, isolated from only four sites of Middle Devonian rocks, and this result remains

unconfirmed by field tests. The directions, however, are unlike those expected for any younger period. Other directions in these Devonian rocks are interpreted as late Paleozoic remagnetizations. Also remagnetized are most Silurian redbeds; in contrast, a bipolar remanence isolated from Early Silurian volcanics is most probably primary as indicated by the positive tilt and conglomerate tests. Summary formation-mean directions, statistical parameters, and paleomagnetic pole positions for the Chingiz Range (this paper and Collins et al., 2003) are listed in Table 3.

The north- and upward-directed Middle Devonian result is clearly reversed. Analysis of possible polarity options suggests that the south-southwestward-pointing Early Silurian direction is of normal polarity, and the same applies to the early Paleozoic southeasterly directions from a nearby part of the Chingiz Range (Collins et al., 2003). Working on this assumption, the Chingiz Range is shown to move in general accord with the Siberian plate, which in turn is in agreement with the Kipchak Arc model for the UMB (Sengör and Natal'in, 1996). Moreover, the succession of paleomagnetic directions from the Chingiz Range generally agrees with this model; it predicts not only latitudinal displacements but rotations as well. This conclusion is not yet corroborated for other parts of the Kazakhstan orocline; our recent paleomagnetic studies of the North Tien Shan reveal a declination pattern, possibly complicated by (block?) rotations within the North Tien Shan zone, that does not match that predicted by the Sengör and Natal'in model. The most general finding of our recent studies is that the UMB units likely moved coherently with Baltica and/or Siberia.

Acknowledgements

We are indebted to many persons from the Scientific Station of the Institute for High Temperatures of the Russian Academy of Sciences in Bishkek (Kyrgyzstan) who helped us organize and carry out the field work in Kazakhstan. We thank Nina Dvorova for paleomagnetic measurements and appreciate the very helpful comments of Vadim Kravchinsky and an anonymous reviewer. This study is supported by the U.S. National Science Foundation, Division of Earth Sciences, grant EAR-9909231, and by the Russian Foundation of Fundamental Research, grants 00-05-64149 and 00-05-64646.

References

- Allen, M.B., Sengör, A.M.C., Natal'in, B.A., 1995. Junggar, Turfan and Alakol basins as Late Permian to? Early Triassic extensional structures in a sinistral shear zone in the Altaid orogenic collage, Central Asia. *J. Geol. Soc., London* 152, 327–338.
- Bandaletov, S.M., 1969. The Silurian of Kazakhstan. Nauka, Alma-Ata. 149 pp. (in Russian).
- Bazhenov, M.L., Collins, A.Q., Degtyarev, K.E., Levashova, N.M., Mikolaichuk, A.V., Pavlov, V.E., Van der Voo, R., 2003. Paleozoic northward drift of the North Tien Shan (Central Asia) as revealed by Ordovician and Carboniferous paleomagnetism. *Tectonophysics* 366, 113–141.
- Bekzhanov, G.R., Koshkin, V.Y., Nikitchenko, I.I., Skrinnik, L.I., Azizov, T.M., Timush, A.V., 2000. Geological structure of Kazakhstan. Acad. Mineral Resources of Republic of Kazakhstan, Almaty. 394 pp. (in Russian).
- Burtman, V.S., Gurary, G.Z., Belenky, A.V., Kudasheva, I.A., 1998. Kazakhstan and the Altai in the Devonian: paleomagnetic evidence. *Geotectonics* 6, 63–71.
- Channell, J.E.T., Lowrie, W., Medizza, F., Alvarez, W., 1978. Paleomagnetism and tectonics in Umbria, Italy. *Earth Planet. Sci. Lett.* 39, 199–210.
- Collins, A.Q., Degtyarev, K.E., Levashova, N.M., Bazhenov, M.L., Van der Voo, R., 2003. Early Paleozoic paleomagnetism of East Kazakhstan: implications for paleolatitudinal drift of tectonic elements within the Ural–Mongol belt. *Tectonophysics* 377, 229–247 (this issue).
- Degtyarev, K.E., 1999. Stratigraphy and structure of Lower Paleozoic carbonate–siliceous–terrigenous complex of the Chingiz Range (East Kazakhstan). *Stratigr. Geol. Correl.* 7, 93–99.
- Degtyarev, K.E., 2003. The position of the Aktau–Junggar microcontinent in the Paleozooids of Central Kazakhstan. *Geotectonics* 37 (4), 14–34.
- Degtyarev, K.E., Ryazantsev, A.V., 1993. Geology of the orogenic Silurian and the structures with continuous sections in the Caledonides of Kazakhstan. In: Milanovsky, E.E. (Ed.), *Geology and Metallogeny of Central Kazakhstan*. Nauka, Moscow, pp. 64–82 (in Russian).
- Didenko, A.L., Morozov, O.L., 1999. Geology and paleomagnetism of Middle–Upper Paleozoic rocks from the Saur Range. *Geotectonics* 4, 64–80.
- Didenko, A.L., Mossakovsky, A.A., Pechersky, D.M., Ruzhentsev, S.V., Samygin, S.G., Kheraskova, T.N., 1994. Geodynamics of Paleozoic oceans of Central Asia. *Geol. Geofiz.* 35 (7–8), 118–145 (in Russian).
- Fisher, R.A., 1953. Dispersion on a sphere. *Proc. R. Soc. Lond., A* 217, 295–305.
- Grishin, D.V., Pechersky, D.M., Degtyarev, K.E., 1997. Paleomagnetism and reconstruction of Middle Paleozoic structure of Central Kazakhstan. *Geotectonics* 1, 71–81.
- Kirschvink, J.L., 1980. The least-square line and plane and the analysis of palaeomagnetic data. *Geophys. J. Roy. Astron. Soc.* 62, 699–718.
- Kurchavov, A.M., 1994. The lateral variability and evolution of orogenic volcanism in the fold belts. *Geotectonics* 28 (2), 3–18.
- Kurchavov, A.M., Baskina, V.A., Bakhteev, M.K., Mossakovsky, A.A., 1999. Geodynamic and paleotectonic interpretation of petrochemical zonation of volcanic belts. *Geotectonics* 33 (1), 64–80.
- Levashova, N.M., Degtyarev, K.E., Bazhenov, M.L., Collins, A.Q., Van der Voo, R., 2003. Permian paleomagnetism of East Kazakhstan and the amalgamation of Eurasia. *Geophys. J. Int.* 152, 677–687.
- Lyons, J.J., Coe, R.S., Zhao, X.X., Renne, P.R., Kazansky, A.Y., Izokh, A.E., Kungurtsev, L.V., Mitrokhin, D.V., 2002. Paleomagnetism of the early Triassic Semeitau igneous series, eastern Kazakhstan. *J. Geophys. Res.* 107 (B7) (10.1029/2001JB000521).
- Mardia, K.V., 1972. *Statistics of Directional Data*. Academic Press, London (357 pp.).
- McFadden, P.L., Reid, A.B., 1982. Analysis of paleomagnetic inclination data. *Geophys. J. Roy. Astron. Soc.* 69, 307–319.
- McFadden, P.L., McElhinny, M.W., 1988. The combined analysis of remagnetization circles and direct observations in paleomagnetism. *Earth Planet. Sci. Lett.* 87, 161–172.
- McFadden, P.L., McElhinny, M.W., 1990. Classification of the reversal test in paleomagnetism. *Geophys. J. Int.* 103, 725–729.
- Miller, W.R., Tauxe, L., Constable, C.G., Staudigel, H., Johnson, S., Constable, S., 2000. When lightning strikes: paleomagnetic data from the San Francisco volcanics. *EOS Trans. AGU* 81 (48), F350 (Fall Meeting Suppl.).
- Montigny, R., Edell, J.B., Thuizat, R., 1981. Oligo-Miocene rotation of Sardinia: K–Ar ages and paleomagnetic data of Tertiary volcanics. *Earth Planet. Sci. Lett.* 54, 261–271.
- Nikitin, I.F., 1972. *The Ordovician of Kazakhstan*, vol. 1. Stratigraphy Nauka, Alma-Ata. 242 pp. (in Russian).
- Opdyke, N.D., Channell, J.E.T., 1996. *Magnetic stratigraphy*. International Geophysics Series, vol. 64. Academic Press, London. 346 pp.
- Palmer, A.R., 1983. The decade of North American geology (DNAG) 1983 geologic time scale. *Geology* 11, 503–504.
- Samygin, S.G., 1974. The Chingiz strike–slip fault and its position

- in the structure of Central Kazakhstan. Nauka, Moscow. 208 pp. (in Russian).
- Sengör, A.M.C., Natal'in, B.A., 1996. Paleotectonics of Asia: fragments of a synthesis. In: Yin, A., Harrison, M. (Eds.), *The Tectonic Evolution of Asia*. Cambridge Univ. Press, Cambridge, pp. 486–640.
- Van der Voo, R., 1993. *Paleomagnetism of the Atlantic, Tethys and Iapetus oceans*. Cambridge Univ. Press, Cambridge. 411 pp.
- Zijderveld, J.D.A., 1967. AC demagnetization of rocks: analysis of results. In: Collinson, D.W., Creer, K.M. (Eds.), *Methods in Paleomagnetism*. Elsevier, Amsterdam, pp. 254–286.